Original Paper: Endocrine Stomach

Digestion

Digestion 2002;65:87–102

Received: July 16, 2001
Accepted: November 21, 2001

Tumor Necrosis Factor-Alpha Effects on Rat Gastric Enterochromaffin-Like Cells

Christian Huber Robert Zanner Agnes Pohlinger Sabine Mahr Bruno Neu Christian Prinz

Department of Medicine II, Technical University of Munich, Germany

Key Words
Apoptosis · Electrophoretic mobility shift assay · Interferon-γ · Nuclear factor κB · Inducible nitric oxide synthase · N^G-Monomethyl-*L*-arginine acetate

Abstract
Gastric enterochromaffin-like (ECL) cells are histamine-producing cells in the gastric epithelium which are responsible for the peripheral regulation of acid secretion. The gastric mucosa is frequently infected with *Helicobacter pylori*, leading to increased levels of the pro-inflammatory cytokine tumor necrosis factor-α (TNF-α). The aim of our current study was to identify the effect of TNF-α on programmed cell death. ECL cells were isolated from the rat corpus mucosa to a purity >90%. TNF receptor and adapter protein presence were determined using RT-PCR, Western blot and immunocytochemistry. Apoptosis was measured by Tdt-mediated dUTP nick end labeling reaction and by DNA fragmentation based ELISA. Isolated ECL cells were found to express the TNF receptor p55 and IFN-γ receptor, but not the TNF receptor p75 or CD95. TNF-α (25 ng/ml) increased apoptosis in ECL cells approximately 4-fold, IFN-γ had no effect. Western blot analysis revealed that TNF-α caused degradation of IκBα within 10 min. EMSA demonstrated that TNF-α led to increased DNA-binding activity of NFκB and that proteasome inhibitors counteracted NFκB activation. Proteasome inhibitors, specific antisense oligodeoxynucleotides against the p65 subunit of the NFκB complex and the NO synthase inhibitor N^G-monomethyl-*L*-arginine completely prevented TNF-α-induced apoptosis. Our data suggest that TNF-α induces apoptosis of isolated gastric ECL cells via activation of NFκB and the generation of NO.

Copyright © 2002 S. Karger AG, Basel

Introduction

Enterochromaffin-like (ECL) cells are histamine-containing neuroendocrine cells in the gastric oxyntic mucosa. This cell type plays an important role for the regulation of acid secretion by releasing histamine as a paracrine stimulant. The importance of ECL cells during pathophysiological changes is poorly understood. The stomach, however, is frequently infected with the bacterium *Helicobacter pylori*, leading to increased mucosal levels of pro-inflammatory cytokines such as tumor necrosis factor (TNF)-α or interleukin (IL)-1β. These cytokines are released in the gastric mucosa from human monocytes and macrophages and may also influence the secretory and proliferative response of ECL cells [1].

Previous studies using isolated gastric ECL cells have determined that histamine release and synthesis are inhibited by the pro-inflammatory cytokine IL-1β [2]. These studies underlined that IL-1β induces programmed cell death of ECL cells via expression of inducible nitric

KARGER

Fax + 41 61 306 12 34
E-Mail karger@karger.ch
www.karger.com

© 2002 S. Karger AG, Basel
0012–2823/02/0652–0087$18.50/0

Accessible online at:
www.karger.com/journals/dig

PD Dr. Christian K. Prinz
II. Medizinische Klinik, Technische Universität München
Ismaningerstrasse 22
D–81675 Munich (Germany)
Tel. +49 89 4140 4073, Fax +49 89 4140 7366, E-Mail christian.prinz@lrz.tum.de

oxide (NO) synthase (iNOS) and bax protein [1]. IL-1β-induced apoptosis of ECL cells may explain the clinical observation that *Helicobacter pylori*-positive patients have significantly lower gastric histamine concentrations and histidine decarboxylase (HDC) activity than *H. pylori*-negative subjects [3–5]. Further mechanisms behind IL-1β inhibition of acid secretion might involve direct inhibition of parietal cells (PC) [6–8], and also stimulation of prostaglandin synthesis [9–11] which in turn inhibits acid secretion. A direct IL-1β effect on ECL cells may be responsible for the hypochlorhydria observed in patients with polymorphisms of the IL-1β promoter. Patients with mutations in the IL-1β promoter sequence are associated with heightened cytokine levels and decreased gastric acidity, but a significantly increased risk for gastric adenocarcinoma [12]. These observations suggest that ECL cells are an important target for pro-inflammatory cytokines present during chronic gastric inflammation which may be of clinical relevance for gastric carcinogenesis.

It is therefore of special interest to investigate the effect of these cytokines on ECL cell function. The prototype of a pro-inflammatory cytokine is TNF-α, which is significantly increased during chronic infection with *H. pylori*. The degree of mucosal TNF-α levels correlates with colonization density as well as with histological alterations in the mucosa [13]. However, little is known about the effect of TNF-α on gastric acid secretion, and especially on ECL cells. TNF-α is a key mediator during chronic inflammation of the human body, i.e. in Crohn's disease or rheumatoid arthritis. Treatment with chimeric TNF-α antibodies as well as soluble TNF receptors significantly improves the course of these diseases, underlining the pathophysiological importance of this cytokine [14–16].

TNF-α is a pleiotropic cytokine which exerts various effects among different tissues. These differences can be explained by the presence of different receptor subtypes, varying signal transduction pathways or different effects of the transcription factors induced by this cytokine. Previous studies have revealed that TNF-α leads to the activation of nuclear factor (NF)κB, yielding in programmed cell death in endocrine cells. In other cell types, however, NFκB activation may have an anti-apoptotic effect and thereby be cytoprotective [17, 18]. It is therefore important to investigate not only receptor presence, but also signal transduction coupled to this protein, since the effect may vary not only among different cell types, but may also be influenced by other growth factors present at the time of stimulation.

The current study was designed to investigate the TNF-α effect on ECL cell apoptosis and the cellular mechanisms promoting this effect. Using isolated ECL cells as an in vitro model, our results clearly show that TNF-α has a direct effect on gastric ECL cells, leading to the activation of NFκB and induction of programmed cell death.

Materials and Methods

Cell Isolation and Primary Cell Culture

Highly enriched ECL cells were prepared as previously described [2, 19]. A total of 80 preparations were used (5 rats per preparation). All sacrifices were performed in accordance with the ethical guidelines of the Technical University of Munich. Local laws, made in 1986, require the announcement of animal killing experiments to the Department of Health of the Government of Oberbayern, Munich, Germany. The experiments comply with all relevant local and institutional regulations. Briefly, the stomachs were treated with pronase E (1.3 mg/ml; Roche, Mannheim, Germany) for enzymatic digestion, the dispersed cells where then subjected to counterflow elutriation (JE-6 elutriation rotor, Beckman Instruments, Palo Alto, Calif.) and density gradient centrifugation (Accudenz, Accurate Chemicals, Westbury, N.J.). Enriched ECL cells were placed on 6-well plates precoated with Matrigel (Becton Dickinson, Heidelberg, Germany; 1:5 dilution). For immunocytochemistry (ICC) and TUNEL assay, 4–5 × 10^4 cells were grown on sterile glass coverslips coated with Cell-Tak (Becton Dickinson; dilution 1:1 with 0.5 *M* $NaHCO_3$). Cells were cultured in DMEM-Ham's F-12 (DMEM/F12), supplemented with 5% FBS, 2% BSA, 10 mg/l gentamycin, 100 n*M* hydrocortisone, and 1 p*M* gastrin. For stimulation experiments, ECL cells were incubated in a Krebs-Ringer solution. ECL cell purity in this cell culture system was greater than 90%, as measured by acridine orange uptake and specific antibody staining using an antibody (Euro Diagnostica, Malmö, Sweden; dilution 1:1,000) against the marker enzyme HDC [19, 20].

Infrequently observed contaminating cells (1–2%) were G, D cells, PC and pepsinogen cells. We therefore actually measured gastrin and somatostatin release in the preparation of highly enriched ECL cells, but we did not obtain measurable concentrations in our preparation at 10^6 cells/ml. The gastrin and somatostatin release was therefore below threshold levels and, therefore, it can be excluded that these hormones interfere with this response. Similarly, the effect of pepsinogen released in minimal, hardly detectable concentrations is unlikely to affect the current results. HCl release from PC is buffered in the culture media as well as incubation media.

Cytokines and substances used for cell stimulation were: recombinant human TNF-α and recombinant rat interferon (IFN)-γ (R&D Systems, Wiesbaden, Germany); the proteasome inhibitors MG132 (Z-Leu-Leu-*L*-leucinal; Bachem AG, Heidelberg, Germany) and proteasome inhibitor I (PSI; N-CBZ-Ile-Glu(o-t-butyl)-Ala-leucinal; Sigma), and the NO synthase (NOS)-inhibitor N^G-monomethyl-*L*-arginine acetate (*L*-NMMA; Sigma).

Immunocytochemistry

For ICC, stainings with an antibody specific for the target protein were performed on glass slides. The culture medium was removed and fixation was carried out in methanol/acetone (1:1) at –20°C for

10 min. After 5 min of lysis in 0.1% Triton X-100, nonspecific binding sites were blocked for 1 h in 10% normal serum matching the species of the secondary antibody. Slides were then incubated with the primary antibody at 4°C overnight, the secondary antibody was added for 1 h at room temperature. All antibody dilutions were made in 2% normal serum. Slides processed without adding the primary antibody served as negative controls. In parallel experiments, slides were stained for the presence of HDC as described previously [21] to visualize ECL cell purity.

Antibodies used were: rabbit anti-TNF receptor type 1 (1:25; Santa Cruz Biotechnology, Santa Cruz, Calif.); mouse anti-CD95 (1:100; Transduction Laboratories, Hamburg, Germany); rabbit anti-IFN-γ receptor (IFN-γ-R) α-chain (1:20; Research Diagnostics; Flanders, N.J.); rabbit anti-IFN-γ-R β-chain (1:20; Research Diagnostics), and FITC-labeled secondary antibodies donkey anti-goat, donkey anti-rabbit and donkey anti-mouse, all at a dilution of 1:50 (Dianova).

Western Blotting

Enriched ECL cells were washed in FBS-supplemented medium, stimulated with vehicle or 25 ng/ml TNF-α over 5 or 10 min, respectively, then washed in PBS. Cells were centrifuged over 10 min at 4°C/14,000 rpm and resuspended in 40 μl of *L*-CAM buffer (1 ml stock solution, 100 μl Triton X-100, 100 μl PMSF [0.5 m*M*] and 8.8 ml H_2O; content of the stock solution: 5 *M* NaCl, 1 *M* KCl, 1 *M* $MgSO_4$, 1 *M* $CaCl_2$, and 1 *M* HEPES in H_2O [pH 7.4]). The lysed cells were kept on ice for 1 h and sonicated; extracts were stored at –20°C until use. Protein concentrations were measured using the Coomassie-blue method developed by Bradford [22] (microassay from Bio-Rad Laboratories, Munich, Germany); a preparation of 10^6 cells yielded approximately 200 μg protein. The conditions used for Western blotting of the TNF receptor (TNF-R) are summarized in table 1. 20–40 μg protein were separated by SDS-PAGE and blotted on PVDF membranes, blocked for 2 h in 10% low fat milk powder in Tris-buffered saline with 0.5% (vol/vol) Tween 20 (TBST) and then incubated with antibodies specific for the inhibitor of NFκB (i.e. IκBα, 1:500, 4°C; New England Biolabs, Beverly, Mass.), TNF-R1 or TNF-associated factor (TRAF)-2 (both from Santa Cruz Biotechnology) overnight. A secondary horseradish peroxidase conjugated antibody (Amersham Pharmacia Biotech, Piscataway, N.J.) was added for 1 h at room temperature and the signals were detected using the ECL system (Amersham Pharmacia Biotech).

Table 1. Conditions used for Western blotting

Protein	SDS gel	Blotting	Primary antibody	Secondary antibody
TNF-R1	10%	1.5 h at 200 mA	1:800	1:1,500
TRAF2	12%	0.75 h at 200 mA	1:1,000	1:1,500
IκBα	12%	1 h at 200 mA	1:500	1:2,000

Reverse Transcriptase-Polymerase Chain Reaction

PCR was performed using a cDNA library prepared from 2×10^7 ECL cells (harvested from 20 preparations) or using freshly isolated RNA, as previously described [20]. The TRIZOL-method (TRIZOL reagent; Gibco BRL, Grand Island, N.Y.) was used to acquire RNA from cultured cells or rat tissues, which was then reverse transcribed (Superscript™; Gibco BRL) to gain cDNA. Primer pairs for PCR yielding TNF-R1, TNF-R2 [23], CD95 [24], IFN-γ-R α chain [25], GAPDH and iNOS [21] were synthesized by MWG Biotech (Ebersberg, Germany). All primers were designed in a way that the amplified sequence spanned at least two different exons to avoid amplification of genomic DNA. The housekeeping gene GAPDH was chosen to determine integrity of the synthesized cDNA.

PCR amplification was performed on an Eppendorf Mastercycler 5330 using Taq MasterMix Kit (Qiagen, Hilden, Germany). Specific primer sequences, annealing temperatures and expected product sizes are shown in table 2. The positions for each of the primers refer to the corresponding NCBI GenBank sequences (TNF-R1, NM-013091; TNF-R2, U55849; CD95, D26112; IFN-γ-R α chain,

Table 2. Parameters for RT-PCR

Product	Primer sequences (sense/antisense)	Position	Temp. °C	Size bp
TNF-R1	5′–aac ccc ggc ttc aac ccc act ctg–3′ 5′–caa agc acg cgg ccc act acg–3′	1,069–1,092 1,535–1,515	63	467
TNF-R2	5′–gat gag aaa tcc cag gat gca gta gg–3′ 5′–tgc tac aga cgt tca cga tgc agg–3′	1–26 256–234	60	256
CD95	5′–caa ggg act gat agc atc ttt gag g–3′ 5′–gtc ctt aac ttt tcg ttc acc agg–3′	119–143 259–236	63	141
IFN-γ-R α-chain	5′–ggt tgg aca aaa aga atc tga cta tgc–3′ 5′–gca ctt ttt acc aca gag agc aag gac–3′	434–460 1,003–977	60	570
GAPDH	5′–tga agg tcg gtg tca acg gat ttg gc–3′ 5′–cat gta ggc cat gag gtc cac cac–3′	35–60 1,017–994	56	983
iNOS	5′–gaa aga act cgg gca tac ct–3′ 5′–ggc gaa gaa caa tcc aca ac–3′	1,848–1,867 2,383–2,402	56	555

NM-010511; GAPDH, NM-017008; iNOS, NM-012611). Reactions were performed by adding 0.5 μl of each primer (20 μ*M*) and 2.5 μl of cDNA. For CD95-PCR, 0.5 μl 50 m*M* $MgCl_2$ were added to a final volume of 25 μl. The reaction consisted of a first cycle of 5 min at 94°C, 1 min at x°C (where x corresponds to the specific annealing temperature) and 1 min at 72°C, 30 amplification cycles (at 94°C, x°C and 72°C, 1 min each) and a last cycle to complete product extension (1 min 94°C, 1 min x°C and 7 min 72°C). PCR amplification for iNOS was performed over 27 cycles. Products were separated by electrophoresis on 2% agarose gels and ethidium bromide staining was visualized using a transilluminator and video documentation system (MWG-Biotech).

Electrophoretic Mobility Shift Assay

Freshly prepared cells, at least 7×10^5 per stimulation, were preincubated at 37°C for 1 h, followed by another hour of stimulation. For preincubation, the cells were incubated in Krebs-Ringer solution and treated with vehicle, the PSI solvent methanol at a final dilution of 1:100, or the specific NFκB inhibitor PSI (6 m*M*). Stimulation was carried out with vehicle or 25 ng/ml of hTNF-α, respectively. After stimulation, all further steps were carried out at 4°C. The cells were centrifuged at 14,000 rpm for 10 min and resuspended in 50 μl of binding buffer (250 m*M* HEPES, 5 m*M* EDTA, 20 m*M* DTT, 40% (vol/vol) glycine and 1 *M* NaCl in 10 × binding buffer). After sonication, whole cell lysates were frozen in liquid nitrogen and stored at –70°C. An aliquot of 5 μl was kept for protein measurement which was performed as described above.

For electrophoretic mobility shift assay (EMSA), 10 μg of whole cell protein in H_2O (ad 20 μl) and 1 × binding buffer were incubated with 4 μg of poly[dI:dC] for 5 min at room temperature; a probe containing no protein served as negative control. Then, 25 ng of cold oligos containing the CREB-consensus sequence or the HIV-NFκB-consensus sequence (Gelshift assay kit; Stratagene, Cambridge, UK), respectively, were incubated 20 min with the lysates of unstimulated cells for competition assay. Finally, 2 μl of ^{32}P-labeled oligos (approximately 100,000 cpm; labeled with T4 polynucleotide kinase, Roche) containing the NFκB-consensus site mentioned above were added to each probe for another 20 min. The extracts were kept on ice, mixed with 2.2 μl of loading buffer (20% Ficoll 400 and 0.25% bromphenol blue in 10× loading buffer) and loaded on a running gel containing 7% of acrylamide in 0.25% TBE running buffer. Electrophoresis was carried out at room temperature for 5–7 h. After the run was completed, the gel was washed, dried, and exposed to either an X-ray film at –70°C for 2–5 days or to a Phosphor Screen (Molecular Dynamics; Sunnyvale, Calif.) for approximately 1 day.

Transfection with Antisense-Phosphorothioate Oligodeoxynucleotides

Transfection of ECL cells was performed as described before [26]. Antisense (AS) oligonucleotides (ODN) spanning the translation initiation codon were constructed for NFκB subunit p65 (5′-ggg gaa cag ttc gtc cat ggc-3′). Missense (MS) ODN (5′-ggg gcg atg agg cct act atc -3′) had an identical nucleotide content in random order and served as negative control. ODN were synthesized in a phosphorothioate-modified form by MWG Biotech. For the use in internalization studies, ODN were 5′-labeled with 6-FAM (6-carboxyfluorescein). Freshly prepared ECL cells were grown on Cell-Tak-coated slides at a density of 1×10^5 cells per slide in culture media over 24 h to allow recovery. Subsequently, culture medium was renewed and cells were incubated at 37°C over 5 h with 10 μ*M* FAM-labeled, AS- or MS-ODN. Transfection efficacy was examined with FAM-labeled ODN by fluorescence microscopy. More than 88% of the cells showed green fluorescent staining in the nuclear region.

Determination of ECL Cell Apoptosis

To determine ECL cell apoptosis, two different techniques were applied. First, we used the in situ cell death detection kit (POD; Roche), which is based on the TUNEL reaction. For this experiment, cells were first grown on glass slides for 24 h as described, then the medium was supplemented with vehicle or cytokines of interest and cells were grown for another 24, 48 or 72 h. In experiments with the specific NFκB inhibitors PSI (6 m*M*) or MG132 (5 m*M*), the cells were pretreated with medium, methanol (1:100) or inhibitor for 1 h, then the cytokines of interest were added for 1 additional hour. After appropriate time, the stimulation was ended by fixation in Bouin's solution over 15 min. Cells were lysed and processed as recommended to block nonspecific binding sites and destroy endogenous peroxidase activity. Incubation with biotinylated deoxynucleotides allowed terminal transferase-mediated labeling of ECL cell DNA strand breaks caused by apoptosis. A peroxidase reaction (Vector Laboratories, Burlingame, Calif.) was used to stain the labeled cell nuclei for light microscopy. Cells were counted in visual fields containing more than 100 cells; the percentage of apoptotic cells was obtained by dividing the number of cells with positive staining by the total number of cells.

Second, an ELISA kit for the detection of histone-associated DNA fragmentation (cell death detection ELISA; Roche) was used for in vitro detection of ECL cell apoptosis. Cells were grown on Matrigel-coated 6-well plates, then stimulation was carried out similar to the TUNEL assay; ECL cells were trypsinated, washed in PBS, then lysed. The degree of antibody binding was visualized by peroxidase reaction and then measured with an ELISA reader at 405 nm. All determinations were carried out in double. Values were calculated as the percent decrease/increase respective to the basal probe, which was set to 100%.

Statistical Analysis

Results are shown as the mean ± SE. Data were analyzed using ANOVA followed by Student-Newman-Keuls test, where $p < 0.05$ was considered significant. Levene's homogeneity-of-variance test was used to assure that the groups for ANOVA came from populations with equal variances.

Results

ECL Cell Enrichment and Presence of Apoptosis-Related Receptors on ECL Cells

Figure 1A and B give an overview of the actual enrichment process. In figure 1A, light microcopy of enriched ECL cells is shown with a total of 18 cells. In figure 1B, ECL cells were stained with a polyclonal antibody against the marker enzyme HDC. 17 of these cells show positive staining for HDC. In a total of more than 450 cells counted, the average enrichment ranged above 94 ± 2%. The few contaminating cells were PC (1–2%), chief cells (1–2%), and endocrine cells such as gastrin and somato-

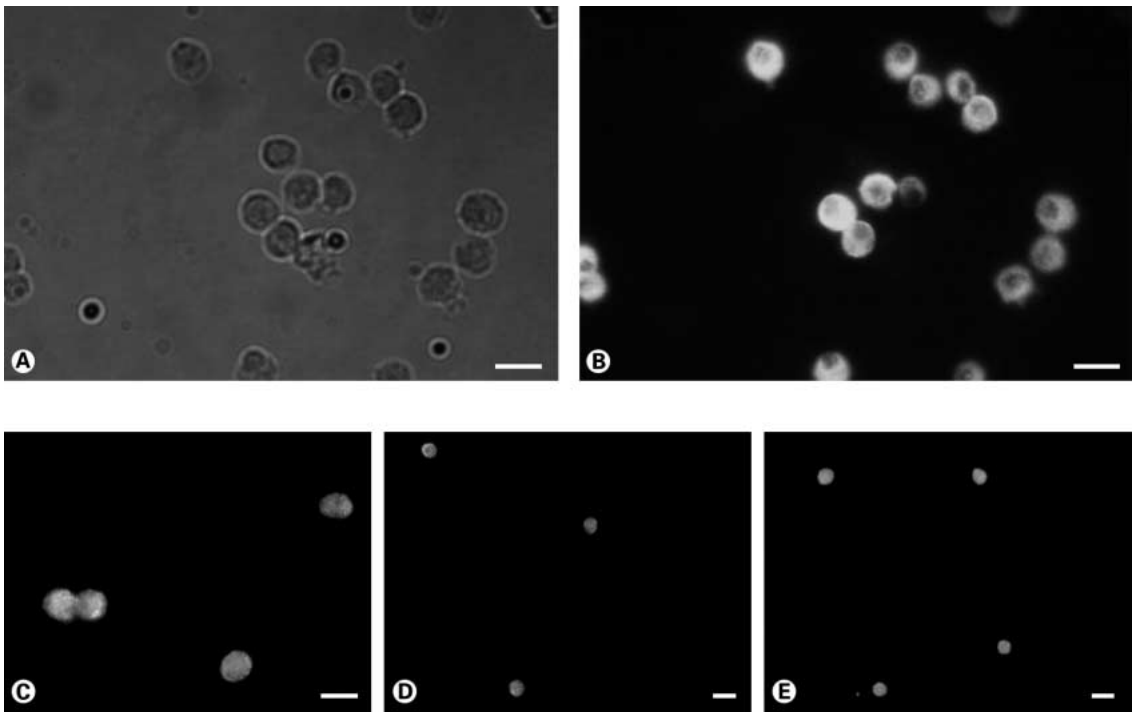

Fig. 1A–E. Immunocytochemistry demonstrating the presence of HDC (A, B), TNF-R1 (C), IFN-γ-R α chain (D) and IFN-γ-R β chain (E) in ECL cells. Immunocytochemistry of ECL cells performed with antibodies specific for HDC (A light microscopy; B antibody staining; ×100), TNF-R subtype 1 (C ×100), IFN-γ-R α chain (D ×37), and IFN-γ-R β chain (E ×37). FITC-labeled secondary antibodies were used to visualize the binding of the primary antibodies. The cells have the typical morphological features of ECL cells and are about 10 μm in size. A total of 3 different experiments was performed yielding identical results. Size bar 10 μm.

statin cells (1–2%). Thus, the total amount of these cells was extremely low. These results are in accordance with previous studies established by our own group [19, 21]. No staining was observed in cells treated without primary antibody (negative controls).

The presence of TNF-R1 as well as of the IFN-γ receptor chain α and β was determined in ECL cells using ICC. ECL cells showed positive staining with antibodies specific for the TNF-R1 (fig. 1C). However, no staining was observed with an antibody specific for the TNF-R2, indicating that this subtype is not present (not shown). Furthermore, the presence of the CD95 receptor (Fas death receptor) was investigated by ICC. No staining could be detected in three repetitive experiments (not shown). In contrast, ECL cells were found to express the α and β chain of the IFN-γ receptor (fig. 1D and E, respectively). ICC was performed on highly purified ECL cells, and demonstrated that the staining for TNF-R1 was homogenous. More than 90% of all cells showed positive staining for all receptor subtypes. A total of 218 cells were counted, yielding more than 200 TNF-R-positive cells. Simultaneous staining for the HDC and TNF-R or IFN-γ-R could not be performed. Nevertheless, all cells that were found to be positive for the TNF and IFN-γ receptors had the typical morphology of ECL cells with a size of 10 μm, a large nucleus and numerous secretory vesicles.

Presence of TNF-R1 and TRAF2 in ECL Cells

PCR was performed with a cDNA library and freshly prepared RNA from ECL cells (fig. 2A–C). In accordance with the results obtained with ICC, PCR gave single products at the expected sizes for the TNF-R1 (fig. 2A) and IFN-γ-R α chain (fig. 2B), but not for the TNF receptor subtype 2 (fig. 2C) or CD95 (not shown). PCR was repeated twice which yielded identical results. The results are shown for the amplification with the cDNA library. These results were identical to the amplifications using RNA from highly enriched ECL cells (purity >94%).

In order to show the presence of TNF-R1 and TRAF2 (an important adapter protein for the NFκB pathway) at

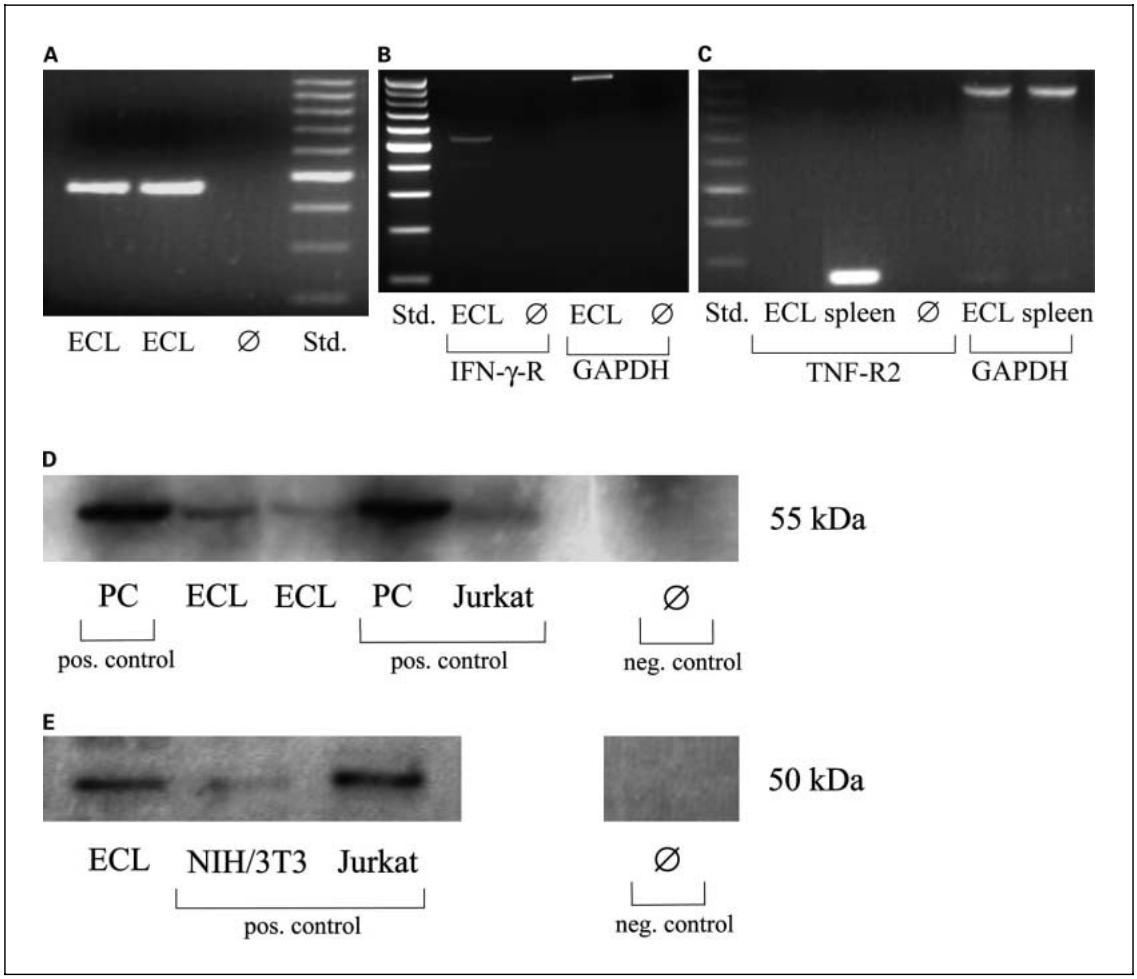

Fig. 2. Detection of TNF-R, IFN-R and TRAF-2 in ECL cells. RT-PCR for TNF-R1(A), IFN-γ-R α-chain (B) and TNF-R2 (C). Rat ECL cell cDNA (ECL) and rat spleen cDNA (spleen) were used as template. Ø = Negative control without cDNA; Std. = molecular weight standard, lanes represent steps of 100 bp where the bright lane equals 500 bp. GAPDH presence was used as a control. Western blot detection of TNF-R1(D) and Western blot detection of TRAF2 protein (E). Protein extracts used were from ECL cells (ECL), Jurkat cells (Jurkat), rat gastric parietal cells (PC) and Swiss/3T3 cells (NIH/3T3). Ø = Negative control.

the protein level, Western blotting with specific antibodies was performed using protein extracts from enriched ECL cells. Figure 2D shows a Western blot for TNF-R1. A strong signal was detected at 55 kD with lysates from PC that served as positive control. Jurkat cell protein used as a second positive control gave a weaker signal. The TNF-R1-specific band was also detected in an ECL cell protein probe. No signal was obtained using PC protein incubated without primary antibody (negative control).

A Western blot specific for TRAF2 is shown in figure 2E. TRAF2-presence could be detected in ECL cells as well as Jurkat and Swiss/3T3 cells (positive controls) as a single band at 50 kD. Again, no signal could be detected with the negative control (no primary antibody). All Western blots were repeated at least twice and gave identical results.

Apoptosis of ECL Cells in the Presence of TNF-α

Programmed cell death in ECL cells was determined under basal conditions and after stimulation with varying concentrations of TNF-α. The methods used for apoptosis quantification were the TUNEL reaction (fig. 3A) and a DNA fragmentation ELISA (fig. 3B). All experiments

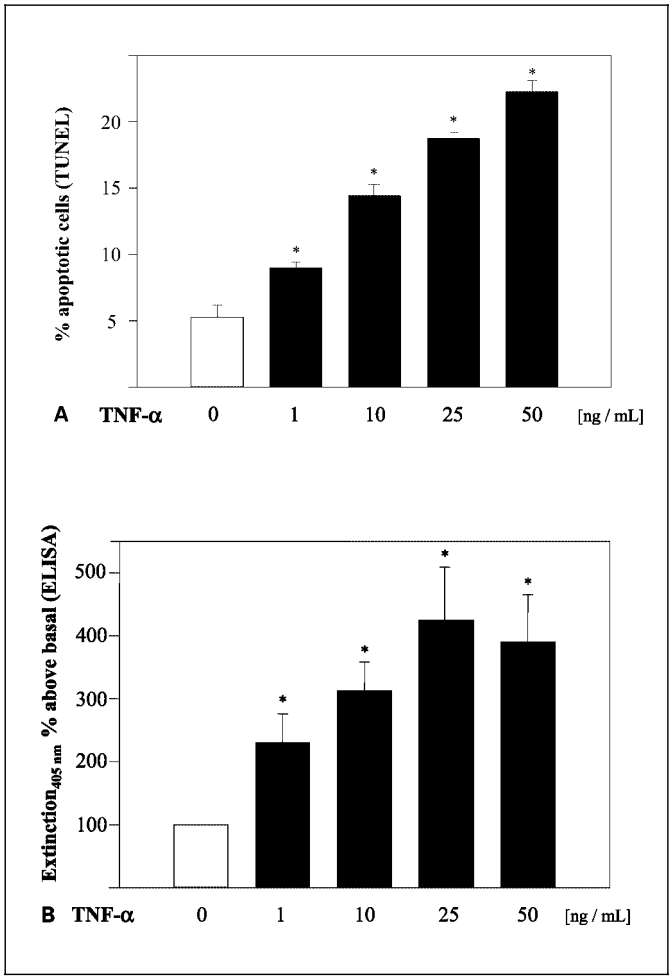

Fig. 3. Percentage of ECL cells undergoing apoptosis after incubation with TNF-α. Apoptosis following incubation with TNF-α (0–50 ng/ml for 24 h) as seen with TUNEL (A) and ELISA (B). Values represent the percentage of apoptotic cells measured by TUNEL or relative extinction at 405 nm in percent measured by ELISA. *Significant differences relative to the apoptotic rate under basal conditions.

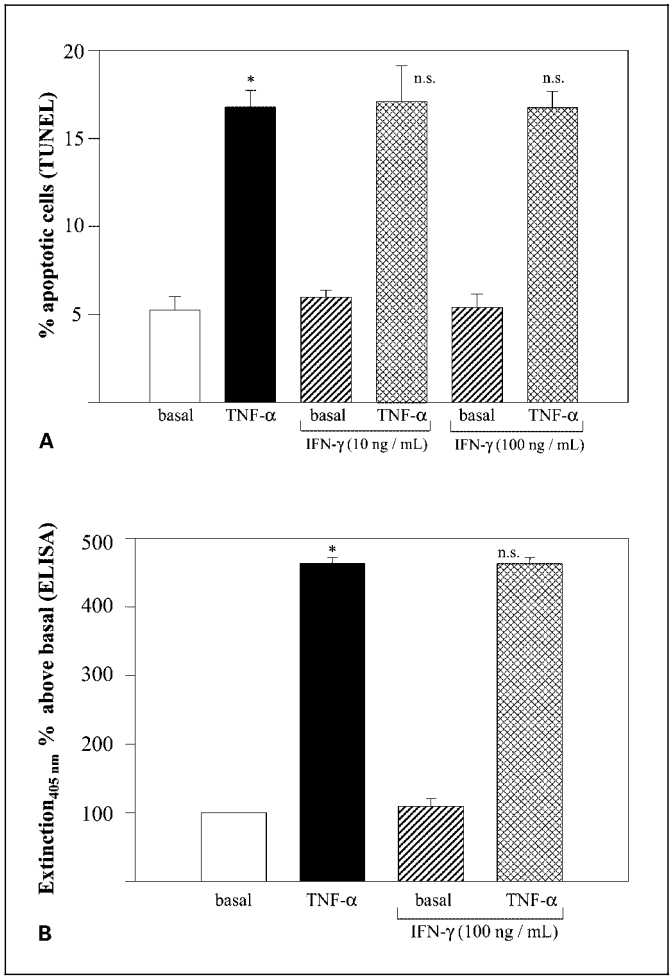

Fig. 4. IFN-γ effects on ECL cells. Apoptosis of ECL cells following simultaneous incubation with TNF-α (25 ng/ml) and/or IFN-γ (10–100 ng/ml) over 24 h as determined by TUNEL (A) or ELISA technique (B). *Significant differences relative to the apoptotic rate under basal conditions. n.s. = Difference was not significant.

were carried out at least three times. Initially, cells were incubated with increasing concentrations of TNF-α (fig. 3A) during a 24-hour incubation period. After 24 h of culture, the basal apoptotic rate of ECL cells ranged between 4 and 6%. 50 ng/ml TNF-α increased the apoptotic rate to 22–24%. All of the indicated concentrations had a highly significant effect ($n = 4$, $p < 0.005$). A similar effect of TNF-α on ECL cell apoptosis was observed using the objective ELISA technique. As shown in figure 3B, TNF-α significantly induced apoptosis at 1, 10, 25 and 50 ng/ml. The highest percentage of programmed cell death was achieved at 25 ng/ml (mean of 400%) and 50 ng/ml (mean of 390%). Therefore, all subsequent experiments were performed with a concentration of 25 ng/ml.

TNF-α effects on ECL cell death during different incubation periods were also determined by TUNEL reaction (not shown). The basal rate of apoptosis did not increase significantly after 48 or 72 h. TNF-α induced apoptosis in a concentration-dependent manner during all time periods tested. However, comparing the overall values, no significant differences between the varying periods were observed. Therefore, a 24-hour interval was chosen in subsequent experiments.

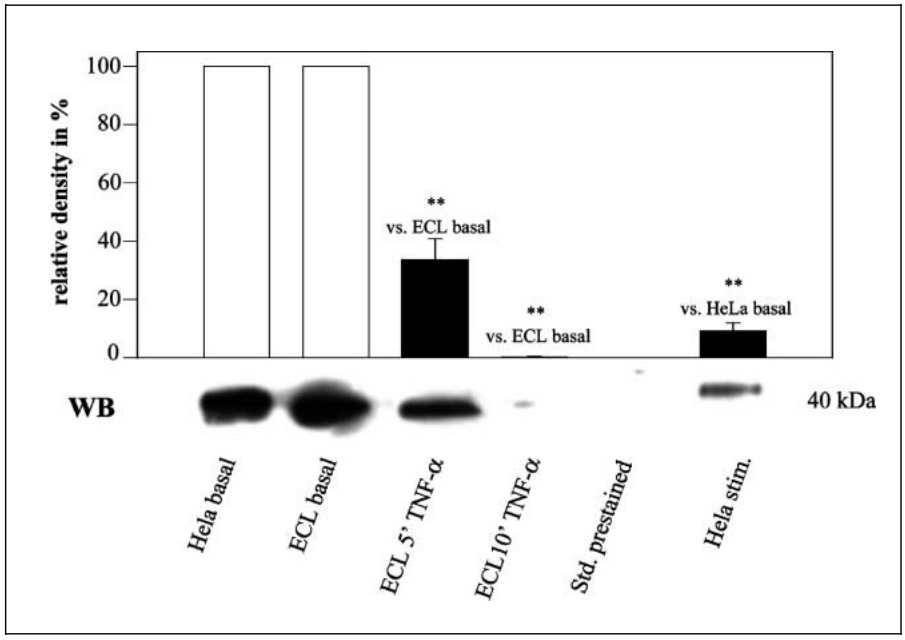

Fig. 5. Time-dependent decrease in the level of IκBα after TNF-α stimulus (Western blot). ECL cells or HeLa cells as control were incubated with TNF-α and protein lysates were incubated with an antibody specific for IκBα. A total of three experiments was performed, the top panel shows the mean optical densities of the specific bands obtained under different conditions. Basal intensity was set to 100%. Lanes 2–4 and the corresponding bars indicate the presence of IκBα at 0 (100%), 5 and 10 min after the addition of TNF-α. Lane 5 contained a prestained standard. HeLa protein extracts without (lane 1, 100%) and after addition of TNF-α (25 ng/ml, lane 6) served as controls. **Significance relative to the corresponding basal signal density. The lower panel shows the actual blot results from one single but representative experiment.

Interferon-γ Effects on ECL Cells

Figure 4 shows the effect of IFN-γ on ECL cells as determined by the TUNEL or ELISA method, respectively. The cells were allowed a 24-hour period of recovery, then vehicle, 10 and 100 ng/ml of IFN-γ were added for 24 h. The basal apoptosis rate ranged from 5 to 6%. IFN-γ did not produce a significant increase of programmed cell death (fig. 4). ECL cells were also subjected to a combined treatment with TNF-α (25 ng/ml) and IFN-γ (10 and 100 ng/ml) for 24 h. TNF-α alone caused 16–18% of apoptosis, but the IFN-γ effects corresponded to the basal level at both concentrations used. Figure 4 shows that the addition of IFN-γ at 10 or 100 ng/ml did not significantly alter the TNF-α effect. Especially, no potentiation of TNF-α effects by the addition of IFN-γ could be observed (total of 3 experiments). Similar results were obtained using the TUNEL and the ELISA technique. A total of 20 experiments was performed.

Degradation of IκBα following TNF-α Stimulation

Following TNF-α stimulation, cytoplasmic IκBα is phosphorylated and degraded within few minutes [27, 28]. To determine this process in our current system, ECL cells were incubated with TNF-α, protein lysates were prepared, and Western blots were performed. The lower panel in figure 5 illustrates the results from representative experiments, yielding a single band at 40 kD. Band intensity was integrated over each individual band. Densitometric analysis was performed based on a total of three experiments. The top panel shows the average densitometric results of three experiments in which the basal amount was set to 100%. TNF reduced intensity significantly ($p < 0.01$, ANOVA test). Lane 1 contains protein from unstimulated HeLa cells with unphosphorylated IκBα. Lane 6 contains protein from TNF-α-treated HeLa cells. These stimulated cells have a smaller amount of IκBα, leading to a weaker signal and serving as a positive control during this experiment. ECL cells were treated with TNF-α for 0, 5 and 10 min and protein lysates were loaded in lanes 2, 3 and 4, respectively. Similar to unstimulated HeLa cells, a very strong band of IκBα was detected in ECL cells at 0 min (lane 2). After 5 min of incubation with TNF-α, the signal already decreased, and at 10 min, no IκBα signal could be detected. Therefore, TNF-α caused rapid phosphorylation, followed by rapid ubiquitination and degradation of IκBα within the first 10 min.

NFκB-Binding Is Enhanced after Incubation with TNF-α

Figure 6A shows an EMSA assay for NFκB performed using whole ECL cell protein extracts. ECL cell lysates were incubated with radioactively labeled ODN containing the NFκB consensus sequence. Lane 1 contains no protein and serves as negative control, lane 2 contains

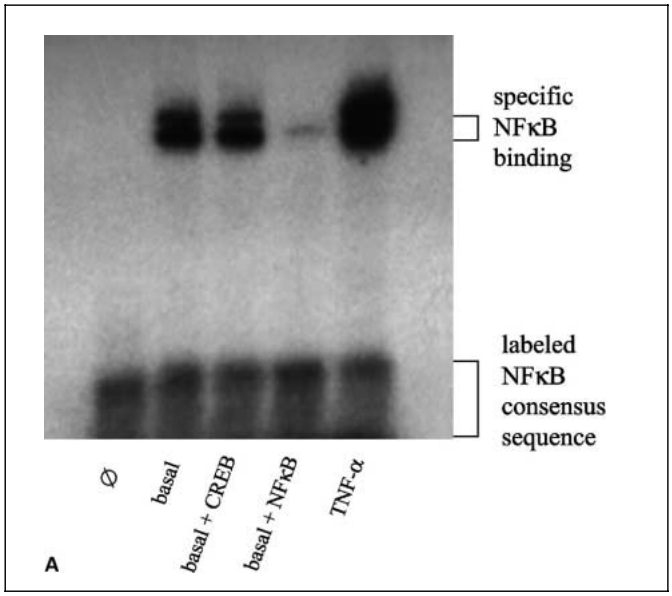

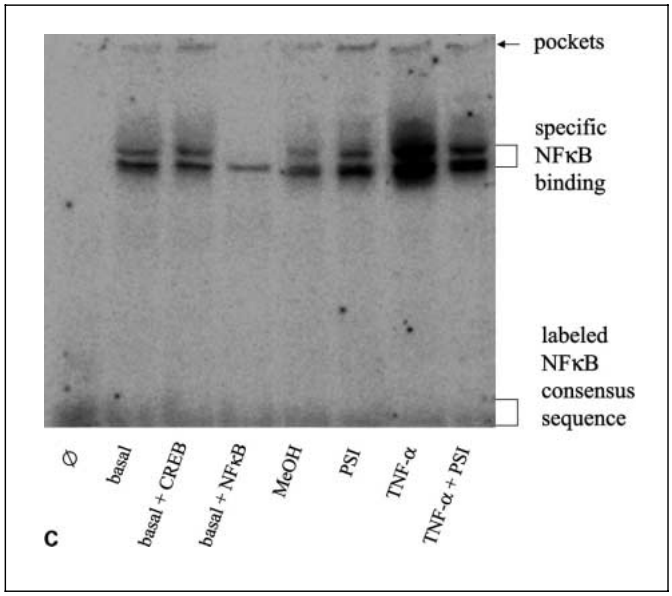

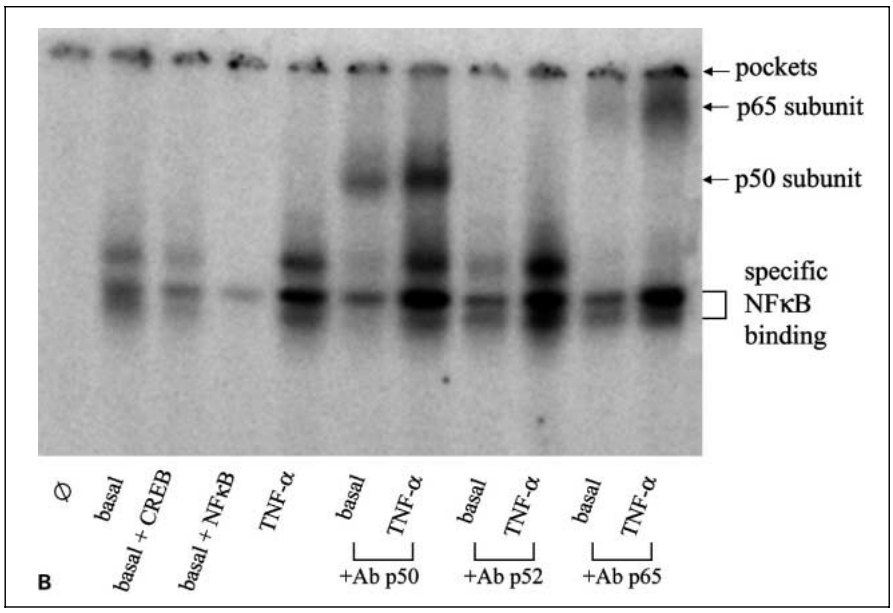

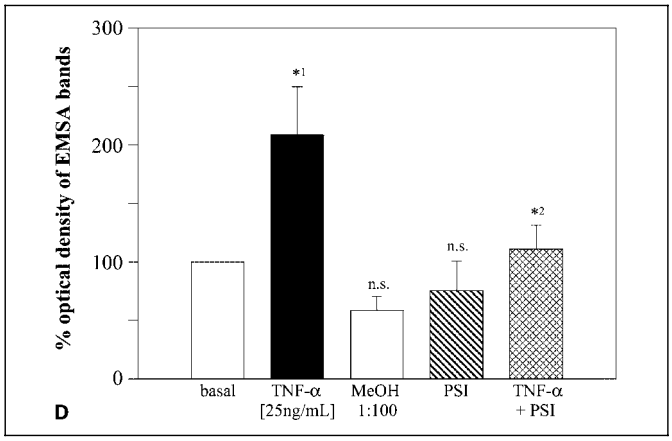

Fig. 6. EMSA of basal or TNF-stimulated ECL whole cell protein lysates. A Stimulation of NFκB activation in ECL cells by TNF-α. Lane 1 = Negative control without protein extract (Ø); lanes 2–4 contain protein lysates from unstimulated cells (basal) incubated in the presence of cold CREB consensus sequence (basal + CREB) or cold NFκB consensus sequence (basal + NFκB, competition assay); lane 5 = protein from TNF-α-stimulated cells (25 ng/ml, 1 h). B Supershift assay by addition of specific NFκB antibodies. Lanes are marked as in figure 7A. In lanes 6–11, antibodies specific for the subunits p50 (+ Ab p50), p52 (+ Ab p52) or p65 (+ Ab p65) were added. A typical supershift could be detected for p50 and p65, the p52 subunit was not detected. C TNF-α-induced NFκB activation is inhibited by PSI. Lanes are marked as in figure 7A. Cells for lanes 5–8 were treated as follows: MeOH = addition of methanol (1:100, 2 h); PSI = addition of PSI (diluted in methanol 1:100, 2 h); TNF-α = pretreatment with methanol (1:100, 1 h), followed by TNF-α (25 ng/ml, 1 h); TNF-α + PSI = pretreatment with PSI (diluted in methanol 1:100 over 1 h), followed by TNF-α (25 ng/ml, 1 h). D Semiquantitative measurement of PSI-induced NFκB activation (EMSA). Bars represent the mean intensity ± SEM of the NFκB-specific signal as measured in three independent assays. *[1]Significant differences relative to the signal in unstimulated and in TNF-stimulated cells. *[2]Difference in TNF-treated cells which were cells treated with TNF and PSI. n.s. = Differences were not significant relative to the basal signal. A one-way ANOVA with subsequent Student-Newman-Keuls test was used to compare the differences.

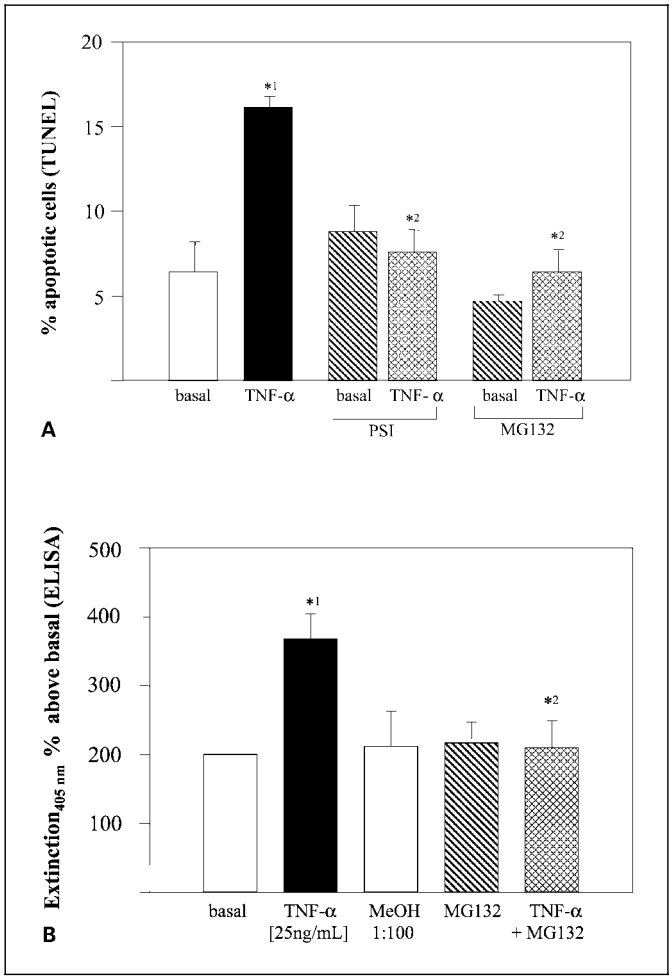

Fig. 7. Effect of PSI and MG132 on ECL cell apoptosis. Measurement of ECL cell apoptosis after incubation with vehicle, vehicle + TNF-α (25 ng/ml, 1 h each), methanol 1% (MeOH, 2 h), the NFκB inhibitors PSI and MG132 (disolved in methanol at a final concentration of 1%, 2 h) and after preincubation with PSI/MG132 (1 h) followed by TNF-α (1 h). Effects were shown using the TUNEL method (PSI, MG132; A) and ELISA (MG132; B). *[1]Significant differences relative to the apoptotic rate under basal conditions. *[2]Significant differences relative to TNF-α-caused apoptosis.

extracts from unstimulated ECL cells. Cell lysates and radioactively labeled NFκB consensus sequence were added together with competing cold CREB consensus sequence (lane 3) or cold NFκB consensus sequence (lane 4). The signal in lane 3 (nonspecific competition) was equal to lane 2, while the signal of lane 4 was strongly reduced (specific competition), proving the specificity of the NFκB-nucleotide interaction in our assay. Lane 5 contains protein from TNF-α-stimulated ECL cells, yielding a much stronger signal compared to basal conditions (lane 2), indicating the TNF-α-induced binding of NFκB to the corresponding consensus sequence in ECL cells.

Subsequently, an EMSA supershift assay was performed (fig. 6B). Samples for lanes 6, 8 and 10 were prepared from basal cell extracts and the ones for lanes 7, 9 and 11 from stimulated cells (three repetitive but independent experiments). In addition, lanes 6 and 7 contain an antibody specific for the p50 subunit of NFκB, lanes 8 and 9 one that recognizes the p52 subunit, and the antibody in lanes 10 and 11 is specific for the p65 subunit. Only in lanes 6 and 7 and 10 and 11 can a band shift be detected. The signal intensity of the shifted bands shows that the activated NFκB mainly consists of the p50 and p65 subunits.

In figure 6C, the effect of the proteasome inhibitor PSI on NFκB activation is shown. The negative control was loaded on lane 1, lane 2 contained basal cell extracts, lane 7 extracts from stimulated cells. In lanes 3 and 4, a competition assay similar to the one in figure 6A was performed. Lanes 5–8 contained extracts from cells treated with methanol, PSI, TNF-α alone and PSI + TNF-α, respectively. Methanol and PSI did not cause activation of NFκB. PSI significantly reduced the TNF-α effect (lane 8), and the resulting band was even weaker than the basal signal.

A total of three independent experiments were performed and results were compared by analyzing the optical densities of the different bands in each experiment (fig. 6D). Addition of methanol or PSI slightly decreased basal NFκB activity (lane 5 vs. lane 2). However, this effect was not statistically significant in 3 experiments using one-way ANOVA.

Effect of Proteasome Inhibitors on TNF-α-Induced Apoptosis

To determine whether NFκB-activation is of functional importance for ECL cell apoptosis in response to TNF-α, we performed a TUNEL assay using two proteasome inhibitors preventing NFκB activation. The PSI is a cell-permeable inhibitor of a multicatalytic proteinase complex that prevents the activation of NFκB in response to TNF-α or IL-1β through inhibition of IκBα degradation, thereby interfering with the induction of iNOS [29]. Similarly, the proteasome inhibitor MG132 has also been shown to prevent proteasomal degradation [30]. The effects of these inhibitors on TNF-α-induced apoptosis are illustrated in figure 7A (TUNEL) and figure 7B (ELISA). 1% methanol was used as solvent for both inhibitors, but had no effect on apoptosis. Cells were incubated with vehicle, TNF-α, the inhibitors, or TNF-α in combi-

nation with PSI or MG132. The basal rate of apoptosis ranged at 7%, and TNF-α caused an increase to 16–18%. PSI or MG132 alone caused no significant change in programmed cell death. However, both inhibitors were able to reduce the percentage of apoptotic cells to 5–8% (as determined by TUNEL; fig. 7A) and thus to completely inhibit TNF-α-induced apoptosis ($n = 3$, $p < 0.01$). Similar results were obtained using the objective ELISA quantification. As shown in figure 7B, TNF-α increased programmed cell death in ECL cells, and MG132 was able to inhibit these effects completely.

Inhibition of TNF-α Induced Apoptosis by p65 AS-ODN and L*-NMMA*

To determine the pro-apoptotic effect of NFκB in detail and to investigate the subsequent steps of signal transduction, ECL cells were incubated in the presence of p65 AS-/MS-ODN and *L*-NMMA. The AS ODN were specific against the p65 subunit of NFκB. Untreated ECL cells as well as ECL cells transfected with AS-/MS-ODN were incubated with vehicle or TNF-α over 24 h and programmed cell death was measured by TUNEL (fig. 8A). AS- and MS-ODN alone did not have a significant effect

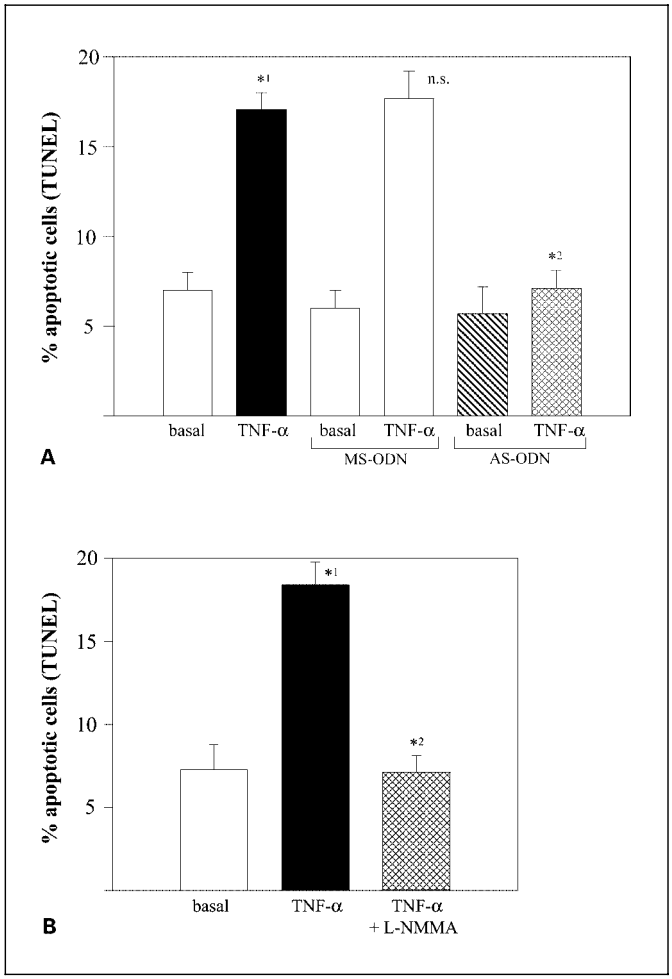

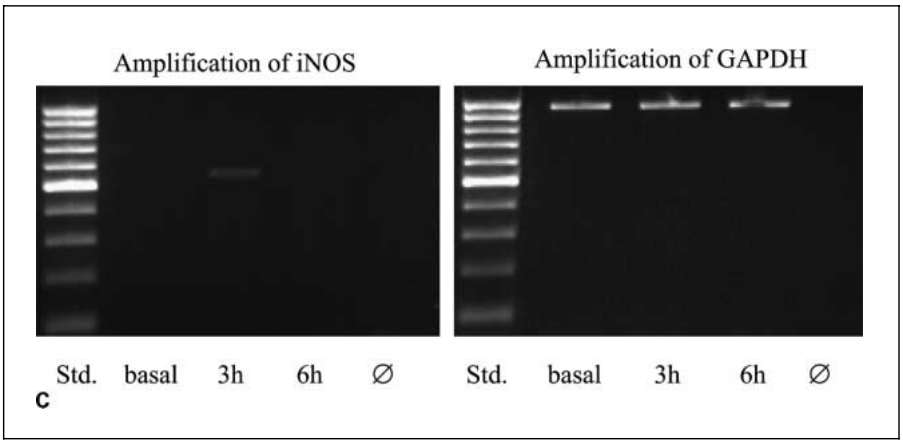

Fig. 8. Effects of p65 AS-ODN and of *L*-NMMA on ECL cell apoptosis. A Effect of NFκB AS-ODN on TNF-α induced ECL cell apoptosis (TUNEL). Cells were treated with vehicle, TNF-α, AS- or MS-ODN, or TNF-α in combination with AS- or MS-ODN at the indicated concentrations. Subsequently, apoptosis was determined using a TUNEL assay and positive cells were counted in percent of all cells seen. Significant results are indicated: *1TNF vs. basal; *2TNF versus TNF+AS-ODN. B *L*-NMMA effect on TNF-α-induced ECL cell apoptosis (TUNEL). Cells were incubated with vehicle, TNF-α (25 ng/ml, 24 h) or TNF-α together with *L*-NMMA (10^{-4} *M*, 24 h). *1Significant differences relative to the apoptotic rate under basal conditions. *2Significant differences relative to TNF-α-caused apoptosis. C RT-PCR for iNOS and GAPDH. RNA from cells incubated with vehicle (lane 2) or with TNF-α (25 ng/ml) for 3 h (lane 3) or 6 h (lane 4) was used. Std. = Molecular weight standard; Ø = negative control for iNOS/GAPDH. Amplification was performed over 27 cycles.

compared to the basal rate of apoptosis. In contrast, transfection with AS-ODN was able to inhibit TNF-α-induced apoptosis completely ($n = 3$, $p < 0.005$). This effect could not be reproduced by preincubation with MS-ODN showing that the decrease in apoptosis was a direct effect of NFκB inhibition.

To determine if this NFκB effect may be dependent on NO generation, TUNEL assays (fig. 8B) were performed with ECL cells incubated with vehicle, TNF-α (25 ng/ml, 24 h) or TNF-α and the specific NOS inhibitor *L*-NMMA (10^{-4} *M*, 24 h). This substance is known to inhibit NO production by all NOS isoforms. Simultaneous incubation with *L*-NMMA and TNF-α was found to inhibit TNF-α-induced cell death completely ($n = 3$, $p < 0.001$). Similar to previous results [1], *L*-NMMA alone did not have an effect on ECL cell apoptosis (not shown).

To further underline the importance of these findings, iNOS induction by TNF-α stimulation was examined by RT-PCR (fig. 8C). The experiment was performed with RNA extracted from unstimulated cells as well as from cells stimulated with TNF-α (25 ng/ml) for 3 and 6 h. Amplification of the housekeeping gene GAPDH yielded identical bands for all three extracts after 27 cycles of amplification, showing that an equal amount of RNA was used for cDNA synthesis. Under basal conditions, no iNOS signal could be detected. After 3 h of TNF-α stimulation, an iNOS signal at 555 bp could be amplified. In RNA from cells incubated with TNF-α for 6 h, the iNOS-specific band disappeared again. This shows a rapid induction of iNOS transcription within the first 3 h of TNF-α stimulation. The results could be reproduced in 2 subsequent experiments.

Discussion

Infection of the gastric mucosa with *H. pylori* leads to chronic inflammation, thereby modulating the secretory and proliferative responses of epithelial as well as endocrine cells [31]. This cytokine is usually absent in the healthy human gastric mucosa. Following infection with *H. pylori*, the expression of TNF-α significantly increases and correlates closely with the degree of *H. pylori* colonization and histological alterations [13]. Simultaneously, chronic *H. pylori* infection is associated with a decrease in acid secretion, which may be due to the effect of the pro-inflammatory cytokines released. Previous studies were unable to show a direct effect of TNF-α on PC [32]. Therefore, TNF-α might also impair histamine secretion from ECL cells, finally leading to decreased gastric histamine secretion, decreased acid secretion and mucosal atrophy. TNF-α has been shown to inhibit function and induce programmed cell death in other neuroendocrine cells, such as thyroid cells [33] or pancreatic β cells [34], and this mechanism may also be of special importance in the gastric mucosa.

Our current data yield clear evidence that ECL cells express the TNF-R1, whereas the TNF-R2 could not be detected. In contrast, we were able to exclude the presence of the CD95 (Fas) receptor in ECL cells using RT-PCR and ICC. The absence of a functional Fas-dependent pathway in ECL cells further underlines the importance of TNF-α and the TNF-R1 during chronic *H. pylori* infection. TNF-R1 is a transmembrane receptor lacking a kinase domain, but containing a so-called death-domain mediating cellular effects. Adapter proteins bearing the death domain bind to the activated receptor and induce several distinct signaling pathways [35–37]. An adapter protein that is associated with the pro-apoptotic action of TNF-R1 is TRAF2. This protein is of special relevance for the TNF-α-mediated activation of NFκB [38–40]. In the current study, we identified TRAF2 in ECL cells by Western blot, underlining the importance of the signaling cascade coupling the stimulation of TNF-R1 to the activation of NFκB.

Incubation of isolated ECL cells with TNF-α led to programmed cell death of ECL cells within 24 h of incubation. TNF-α had a concentration- and time-dependent pro-apoptotic effect, with a 2- to 3-fold increase in apoptosis at a concentration of 25 ng/ml. TUNEL as well as the objective ELISA yielded identical results. The time period observed here and the concentrations used are in accordance with previous studies investigating TNF-α-induced apoptosis in pancreatic tumor cells [41] and gastric epithelial cells [42, 43]. Although only a subgroup of ECL cells (25%) underwent apoptosis in response to TNF-α, this effect may still reflect physiological conditions. First, our data can only detect the status during a short incubation period in vitro, and may become even more evident during life-long infection with the bacteria. ECL cells in vitro and in vivo may be susceptible only at a certain time point during their life cycle (approximately 60 days). Second, TNF-α induction of ECL cell death was significantly higher than the apoptotic rate seen after incubation with the cytokine IL-1β (100 pg/ml, 24 h) in our previous studies [1]. With regard to IL-1β, the physiological importance of this cytokine has already been documented by showing that IL-1β impairs histamine release completely [2]. Furthermore, patients with polymorphisms of the IL-1β promoter have an increased risk of gastric adenocarcinoma

[12]. Since TNF-α and IL-1β are released during chronic inflammation, it appears likely that both cytokines play an important role in the induction of hypochlorhydric conditions.

In addition, we investigated the effects of IFN-γ on ECL cell function. IFN-γ has been shown to potentiate TNF-α-induced apoptosis [41, 44, 45]. We therefore incubated ECL cells with IFN-γ at varying physiological concentrations or with a combination of both TNF-α and IFN-γ. Although we detected the presence of both subunits of the IFN-γ-R, the corresponding ligand did not cause apoptosis alone or together with TNF-α. This could be due to a nonfunctional IFN-γ-R present on ECL cells. Alternatively, the signal transduction pathway activated by IFN-γ may not interfere with that activated by TNF-α. Hence, we investigated the cellular steps mediating the TNF-α effect in our cell system.

TNF-α has been shown to induce various signal transduction pathways, including activation of effector caspases, ceramide production or disruption of the Bcl2/Bax equilibrium [46–48]. TNF-α can also lead to the activation of NFκB. This transcription factor is known to be involved in the regulation of inflammatory as well as survival genes. Thus, we investigated the signal transduction and NFκB induction in detail. Indeed, stimulation with TNF-α led to the activation of NFκB in ECL cells. Following the binding of TRAF2 to TNF-R1, a kinase cascade is activated that results in the phosphorylation of IκB, followed by its ubiquitination and degradation. In our Western blotting experiments, a rapid decrease in IκBα was documented within the first 10 min after stimulation, showing degradation of IκBα as well as activation of NFκB. This finding is consistent with previous studies demonstrating phosphorylation of IκB at Ser32 and Ser36 and subsequent translocation of NFκB to the nucleus following degradation of IκBα [27, 49]. Uncoupling of NFκB from the IκB/NFκB complex was also shown directly using the EMSA method. Because of the small sample volume, we used whole cell extracts instead of nuclear extracts similar to other studies [50, 51]. A strong activation of NFκB within the first hour after stimulation was observed. NFκB in extracts of stimulated as well as unstimulated cells mainly consisted of the subunits p50 and p65. It may be possible that other subunits such as the p52 contribute, at least in part, to the formation of the NFκB complex in ECL cells. Due to the lack of an adequate control for p52, this possibility may not be ruled out, but appears unlikely since a high signal intensity was observed for p50 and p65 in supershift assays.

Subsequently, we investigated the effect of specific proteasome inhibitors that interfered with NFκB activation during ECL cell apoptosis. MG132 and PSI are both specific inhibitors of the chymotrypsin-like activity of the 20S proteasome and are often used to show the functional role of NFκB [30, 52]. They abolish the degradation of phosphorylated IκBα, so that NFκB cannot translocate to the nucleus. Using these inhibitors, TNF-α-caused apoptosis could be totally blocked; furthermore, PSI decreased NFκB binding as shown in EMSA assays. Moreover, transfection experiments demonstrated that specific antisense ODN against the p65 subunit of the NFκB complex completely prevented TNF-α-induced apoptosis, as shown by TUNEL assay. Since the p65 subunit is contained in a high percentage in NFκB heterodimers [17], this subunit appears to be of special importance. Taken together, these experiments suggest a pro-apoptotic role of NFκB during TNF-α-induced apoptosis of ECL cells.

NFκB has been shown to exert different functions, depending on cell type and experimental conditions. NFκB is both able to promote programmed cell death in some tissues or to rescue other cells from apoptosis depending on the varying gene expression [53]. Even in a single cell type, NFκB can exert diverging functions, depending on the experimental conditions [18]. NFκB has been found to inhibit cytokine-induced apoptosis in several cell types [17, 38, 48, 54, 55]. However, a pro-apoptotic effect of NFκB has been documented in a wide range of cell types [56–60]. Decoy ODN containing NFκB-binding sites inhibited virus-induced apoptosis of human hepatoma cells [61] and of a prostate carcinoma cell line [62].

Several previous works have specifically investigated a pro-apoptotic effect of NFκB in response to TNF-α stimulation. TNF-α-induced apoptosis was associated with NFκB activation in myeloid cell lines [63] and in osteoblastic MC3T3-E1 cells [47]. In the work of Kitajima et al [47], activation of NFκB was detected in the perinuclear region after 5 min of TNF-α treatment and translocation into the nucleus was observed within 15 min. Claudio et al. [64] demonstrated a functional association of NFκB with TNF-α-dependent apoptosis. This group observed that WEHI 164 cells treated with TNF-α for up to 6 h can be rescued as long as NFκB relocalizes to the cytoplasm in its inactive form, whereas 15 min of TNF-α stimulation were sufficient to induce apoptosis. These works underline a pro-apoptotic function of this transcription factor in response to TNF-α stimulation, according to our current data. This appears to be a unique feature in gastric ECL

cells, thereby paralleling results observed in pancreatic beta cells.

One pathway activated by NFκB leading to apoptosis may be the generation of NO. In ECL cells, *L*-NMMA prevented TNF-α-induced apoptosis completely, suggesting the importance of NO generation in this process, similar to observations made pancreatic β-cells following IL-1β stimulation [65]. TNF-α has been shown to induce iNOS expression in gastric mucosa [66], but the cellular targets have remained unclear. In β cells, NFκB activation is linked to apoptosis, and this effect appeared to be mediated by induction of iNOS and generation of NO [67]. The promoter region of the rat iNOS gene (GenBank accession number D84101) contains the NFκB consensus sequence (5′-GGRNNYYCC-3′) four times at positions 71–79, 134–142, 888–896 and 930–938, underlining the functional interaction between NFκB activation and iNOS transcription. Our data further support the idea that iNOS is expressed in ECL cells 3 h after TNF-α stimulation, and is thus a key enzyme mediating cytokine-induced ECL cell death, leading to the generation of NO and subsequent apoptosis in ECL cells.

In summary, our data yield evidence that TNF-α has a direct effect on gastric ECL cells, leading to programmed cell death. Activation of NFκB and generation of NO appear to be of special importance for the mediation of ECL cell death. These findings underline that ECL cells are a target for pro-inflammatory cytokines and thereby play a key role in the development of decreased gastric acidity, which may predispose to atrophic gastritis and the development of gastric cancer.

Acknowledgements

We thank Nina Neumayer and Hedda Herrmuth for her competent help with many of the applied techniques. This work was supported by Deutsche Forschungsgemeinschaft (grant Pr 411/2–2 and 411/9–1) and by Gastrofoundation, Munich. C. Prinz is the recipient of the Heisenberg Award of the Deutsche Forschungsgemeinschaft (Pr 411/7–1).

References

1 Mahr S, Neumayer N, Gerhard M, Classen M, Prinz C: IL-1beta-induced apoptosis in rat gastric enterochromaffin-like cells is mediated by iNOS, NF-kappaB, and Bax protein. Gastroenterology 2000;118:515–524.
2 Prinz C, Neumayer N, Mahr S, Classen M, Schepp W: Functional impairment of rat enterochromaffin-like cells by interleukin 1 beta. Gastroenterology 1997;112:364–375.
3 Queiroz DM, Mendes EN, Rocha GA, Cunha-Melo JR, Barbosa AJ, Lima GF Jr, Oliveira CA: *Helicobacter pylori* and gastric histamine concentrations. J Clin Pathol 1991;44:612–613.
4 Queiroz DM, Mendes EN, Rocha GA, Barbosa AJ, Carvalho AS, Cunha-Melo JR: Histamine concentration of gastric mucosa in *Helicobacter pylori* positive and negative children. Gut 1991;32:464–466.
5 Queiroz DM, Mendes EN, Rocha GA, Moura SB, Resende LM, Cunha-Melo JR, Coelho LG, Passos MC, Oliveira CA, Lima GF Jr: Histamine content of the oxyntic mucosa from duodenal ulcer patients: Effect of *Helicobacter pylori* eradication. Am J Gastroenterol 1993;88:1228–1232.
6 Schepp W, Dehne K, Herrmuth H, Pfeffer K, Prinz C: Identification and functional importance of IL-1 receptors on rat parietal cells. Am J Physiol 1998;275:G1094–G1105.
7 Beales IL, Calam J: Interleukin 1 beta and tumour necrosis factor alpha inhibit acid secretion in cultured rabbit parietal cells by multiple pathways. Gut 1998;42:227–234.
8 Nompleggi DJ, Beinborn M, Roy A, Wolfe MM: The effect of recombinant cytokines on [^{14}C]-aminopyrine accumulation by isolated canine parietal cells. J Pharmacol Exp Ther 1994;270:440–445.
9 Lindstrom E, Hakanson R: Prostaglandins inhibit secretion of histamine and pancreastatin from isolated rat stomach ECL cells. Br J Pharmacol 1998;124:1307–1313.
10 Uehara A, Okumura T, Sekiya C, Okamura K, Takasugi Y, Namiki M: Interleukin-1 inhibits the secretion of gastric acid in rats: Possible involvement of prostaglandin. Biochem Biophys Res Commun 1989;162:1578–1584.
11 Robert A, Olafsson AS, Lancaster C, Zhang WR: Interleukin-1 is cytoprotective, antisecretory, stimulates PGE2 synthesis by the stomach, and retards gastric emptying. Life Sci 1991;48:123–134.
12 El-Olmar EM, Carrington M, Chow WH, McColl KE, Bream JH, Young HA, Herrera J, Lissowska J, Yuan CC, Rothman N, Lanyon G, Martin M, Fraumeni JF Jr, Rabkin CS: Interleukin-1 polymorphisms associated with increased risk of gastric cancer. Nature 2000;404:398–402.
13 Yamaoka Y, Kita M, Kodama T, Sawai N, Kashima K, Imanishi J: Induction of various cytokines and development of severe mucosal inflammation by cagA gene positive *Helicobacter pylori* strains. Gut 1997;41:442–451.
14 Maini R, St Clair EW, Breedveld F, Furst D, Kalden J, Weisman M, Smolen J, Emery P, Harriman G, Feldmann M, Lipsky P: Infliximab (chimeric anti-tumour necrosis factor alpha monoclonal antibody) versus placebo in rheumatoid arthritis patients receiving concomitant methotrexate: A randomised phase III trial. Lancet 1999;354:1932–1939.
15 Mouser JF, Hyams JS: Infliximab: A novel chimeric monoclonal antibody for the treatment of Crohn's disease. Clin Ther 1999;21:932–942.
16 D'haens G, Van Deventer S, Van Hogezand R, Chalmers D, Kothe C, Baert F, Braakman T, Schaible T, Geboes K, Rutgeerts P: Endoscopic and histological healing with infliximab anti-tumor necrosis factor antibodies in Crohn's disease: A European multicenter trial. Gastroenterology 1999;116:1029–1034.
17 Baeuerle PA, Baltimore D: NF-kappa B: Ten years after. Cell 1996;87:13–20.
18 Lin KI, DiDonato JA, Hoffmann A, Hardwick JM, Ratan RR: Suppression of steady-state, but not stimulus-induced NF-kappaB activity inhibits alphavirus-induced apoptosis. J Cell Biol 1998;141:1479–1487.
19 Prinz C, Scott DR, Hurwitz D, Helander HF, Sachs G: Gastrin effects on isolated rat enterochromaffin-like cells in primary culture. Am J Physiol 1994;267:G663–G675.
20 Prinz C, Sachs G, Walsh JH, Coy DH, Wu SV: The somatostatin receptor subtype on rat enterochromaffinlike cells. Gastroenterology 1994;107:1067–1074.

21 Mahr S, Neumayer N, Kolb HJ, Schepp W, Classen M, Prinz C: Growth factor effects on apoptosis of rat gastric enterochromaffin-like cells. Endocrinology 1998;139:4380–4390.
22 Bradford MM: A rapid and sensitive method for the quantitation of microgram quantities of protein utilizing the principle of protein-dye binding. Anal Biochem 1976;72:248–254.
23 Bader T, Nettesheim P: Tumor necrosis factor-alpha modulates the expression of its p60 receptor and several cytokines in rat tracheal epithelial cells. J Immunol 1996;157:3089–3096.
24 Kimura K, Wakatsuki T, Yamamoto M: A variant mRNA species encoding a truncated form of Fas antigen in the rat liver. Biochem Biophys Res Commun 1994;198:666–674.
25 Neumann H, Schmidt H, Cavalie A, Jenne D, Wekerle H: Major histocompatibility complex (MHC) class I gene expression in single neurons of the central nervous system: Differential regulation by interferon (IFN)-gamma and tumor necrosis factor (TNF)-alpha. J Exp Med 1997;185:305–316.
26 Reuning U, Wilhelm O, Nishiguchi T, Guerrini L, Blasi F, Graeff H, Schmitt M: Inhibition of NF-kappa B-Rel A expression by antisense oligodeoxynucleotides suppresses synthesis of urokinase-type plasminogen activator (uPA) but not its inhibitor PAI-1. Nucleic Acids Res 1995;23:3887–3893.
27 Wang D, Baldwin AS Jr: Activation of nuclear factor-kappaB-dependent transcription by tumor necrosis factor-alpha is mediated through phosphorylation of RelA/p65 on serine 529. J Biol Chem 1998;273:29411–29416.
28 Ding GJ, Fischer PA, Boltz RC, Schmidt JA, Colaianne JJ, Gough A, Rubin RA, Miller DK: Characterization and quantitation of NF-kappaB nuclear translocation induced by interleukin-1 and tumor necrosis factor-alpha. Development and use of a high capacity fluorescence cytometric system. J Biol Chem 1998;273:28897–28905.
29 Griscavage JM, Wilk S, Ignarro LJ: Inhibitors of the proteasome pathway interfere with induction of nitric oxide synthase in macrophages by blocking activation of transcription factor NF-kappa B. Proc Natl Acad Sci USA 1996;93:3308–3312.
30 Jensen TJ, Loo MA, Pind S, Williams DB, Goldberg AL, Riordan JR: Multiple proteolytic systems, including the proteasome, contribute to CFTR processing. Cell 1995;83:129–135.
31 Calam J, Gibbons A, Healey ZV, Bliss P, Arebi N: How does *Helicobacter pylori* cause mucosal damage? Its effect on acid and gastrin physiology. Gastroenterology 1997;113:S43-S49.
32 Tani N, Watanabe Y, Suzuki T, Muramatsu S, Miyazawa M, Kimura N, Miwa T: Effects of inflammatory cytokines induced by *Helicobacter pylori* infection on aminopyrine accumulation in parietal cells isolated from guinea pigs. Dig Dis Sci 1999;44:686–690.
33 Pang XP, Yoshimura M, Hershman JM: Suppression of rat thyrotroph and thyroid cell function by tumor necrosis factor-alpha. Thyroid 1993;3:325–330.
34 Yamada K, Takane N, Otabe S, Inada C, Inoue M, Nonaka K: Pancreatic beta-cell-selective production of tumor necrosis factor-alpha induced by interleukin-1. Diabetes 1993;42:1026–1031.
35 Weiss T, Grell M, Hessabi B, Bourteele S, Muller G, Scheurich P, Wajant H: Enhancement of TNF receptor p60-mediated cytotoxicity by TNF receptor p80:Requirement of the TNF receptor-associated factor-2 binding site. J Immunol 1997;158:2398–2404.
36 Declercq W, Denecker G, Fiers W, Vandenabeele P: Cooperation of both TNF receptors in inducing apoptosis: Involvement of the TNF receptor-associated factor binding domain of the TNF receptor 75. J Immunol 1998;161:390–399.
37 Tartaglia LA, Weber RF, Figari IS, Reynolds C, Palladino MA Jr, Goeddel DV: The two different receptors for tumor necrosis factor mediate distinct cellular responses. Proc Natl Acad Sci USA 1991;88:9292–9296.
38 Lee SY, Kaufman DR, Mora AL, Santana A, Boothby M, Choi Y: Stimulus-dependent synergism of the antiapoptotic tumor necrosis factor receptor-associated factor 2 (TRAF2) and nuclear factor kappaB pathways. J Exp Med 1998;188:1381–1384.
39 Hsu H, Shu HB, Pan MG, Goeddel DV: TRADD-TRAF2 and TRADD-FADD interactions define two distinct TNF receptor 1 signal transduction pathways. Cell 1996;84:299–308.
40 Jobin C, Holt L, Bradham CA, Streetz K, Brenner DA, Sartor RB: TNF receptor-associated factor-2 is involved in both IL-1 beta and TNF-alpha signaling cascades leading to NF-kappa B activation and IL-8 expression in human intestinal epithelial cells. J Immunol 1999;162:4447–4454.
41 Schmiegel WH, Caesar J, Kalthoff H, Greten H, Schreiber HW, Thiele HG: Antiproliferative effects exerted by recombinant human tumor necrosis factor-alpha (TNF-alpha) and interferon-gamma (IFN-gamma) on human pancreatic tumor cell lines. Pancreas 1988;3:180–188.
42 Slomiany BL, Piotrowski J, Slomiany A: Induction of tumor necrosis factor-alpha and apoptosis in gastric mucosal injury by indomethacin: effect of omeprazole and ebrotidine. Scand J Gastroenterol 1997;32:638–642.
43 Takagi A, Watanabe S, Igarashi M, Koike J, Hasumi K, Deguchi R, Koga Y, Miwa T: The effect of *Helicobacter pylori* on cell proliferation and apoptosis in gastric epithelial cell lines. Aliment Pharmacol Ther 2000;14:188–192.
44 Pandita R, Pocsik E, Aggarwal BB: Interferon-gamma induces cell surface expression for both types of tumor necrosis factor receptors. FEBS Lett 1992;312:87–90.
45 Helseth E, Torp S, Dalen A, Unsgaard G: Effects of interferon-gamma and tumor necrosis factor-alpha on clonogenic growth of cell lines and primary cultures from human gliomas and brain metastases. APMIS 1989;97:569–574.
46 Cohen MC, Cohen S: Cytokine function: a study in biologic diversity. Am J Clin Pathol 1996;105:589–598.
47 Kitajima I, Soejima Y, Takasaki I, Beppu H, Tokioka T, Maruyama I: Ceramide-induced nuclear translocation of NF-kappa B is a potential mediator of the apoptotic response to TNF-alpha in murine clonal osteoblasts. Bone 1996;19:263–270.
48 Liu ZG, Hsu H, Goeddel DV, Karin M: Dissection of TNF receptor 1 effector functions: JNK activation is not linked to apoptosis while NF-kappaB activation prevents cell death. Cell 1996;87:565–576.
49 Brown K, Gerstberger S, Carlson L, Franzoso G, Siebenlist U: Control of I kappa B-alpha proteolysis by site-specific, signal-induced phosphorylation. Science 1995;267:1485–1488.
50 Bork PM, Schmitz ML, Kuhnt M, Escher C, Heinrich M: Sesquiterpene lactone containing Mexican Indian medicinal plants and pure sesquiterpene lactones as potent inhibitors of transcription factor NF-kappaB. FEBS Lett 1997;402:85–90.
51 Hehner SP, Heinrich M, Bork PM, Vogt M, Ratter F, Lehmann V, Schulze-Osthoff K, Droge W, Schmitz ML: Sesquiterpene lactones specifically inhibit activation of NF-kappa B by preventing the degradation of I kappa B-alpha and I kappa B-beta. J Biol Chem 1998;273:1288–1297.
52 Figueiredo-Pereira ME, Berg KA, Wilk S: A new inhibitor of the chymotrypsin-like activity of the multicatalytic proteinase complex (20S proteasome) induces accumulation of ubiquitin-protein conjugates in a neuronal cell. J Neurochem 1994;63:1578–1581.
53 Kaltschmidt B, Kaltschmidt C, Hofmann TG, Hehner SP, Droge W, Schmitz ML: The pro- or anti-apoptotic function of NF-kappaB is determined by the nature of the apoptotic stimulus. Eur J Biochem 2000;267:3828–3835.
54 Beg AA, Baltimore D: An essential role for NF-kappaB in preventing TNF-alpha-induced cell death. Science 1996;274:782–784.
55 Van Antwerp DJ, Martin SJ, Kafri T, Green DR, Verma IM: Suppression of TNF-alpha-induced apoptosis by NF-kappaB. Science 1996;274:787–789.
56 Grimm S, Bauer MK, Baeuerle PA, Schulze-Osthoff K: Bcl-2 down-regulates the activity of transcription factor NF-kappaB induced upon apoptosis. J Cell Biol 1996;134:13–23.
57 Jung M, Zhang Y, Lee S, Dritschilo A: Correction of radiation sensitivity in ataxia telangiectasia cells by a truncated I kappa B-alpha. Science 1995;268:1619–1621.
58 Hettmann T, DiDonato J, Karin M, Leiden JM: An essential role for nuclear factor kappaB in promoting double positive thymocyte apoptosis. J Exp Med 1999;189:145–158.
59 Qin ZH, Chen RW, Wang Y, Nakai M, Chuang DM, Chase TN: Nuclear factor kappaB nuclear translocation upregulates c-Myc and p53 expression during NMDA receptor-mediated apoptosis in rat striatum. J Neurosci 1999;19:4023–4033.

60 Nakai M, Qin ZH, Wang Y, Chase TN: Free radical scavenger OPC-14117 attenuates quinolinic acid-induced NF-kappaB activation and apoptosis in rat striatum. Brain Res Mol Brain Res 1999;64:59–68.
61 Marianneau P, Cardona A, Edelman L, Deubel V, Despres P: Dengue virus replication in human hepatoma cells activates NF-kappaB which in turn induces apoptotic cell death. J Virol 1997;71:3244–3249.
62 Lin KI, Lee SH, Narayanan R, Baraban JM, Hardwick JM, Ratan RR: Thiol agents and Bcl-2 identify an alphavirus-induced apoptotic pathway that requires activation of the transcription factor NF-kappa B. J Cell Biol 1995; 131:1149–1161.
63 Hu X, Tang M, Fisher AB, Olashaw N, Zuckerman KS: TNF-alpha-induced growth suppression of CD34+ myeloid leukemic cell lines signals through TNF receptor type I and is associated with NF-kappa B activation. J Immunol 1999;163:3106–3115.
64 Claudio E, Segade F, Wrobel K, Ramos S, Bravo R, Lazo PS: Molecular mechanisms of TNFalpha cytotoxicity: Activation of NF-kappaB nuclear translocation. Exp Cell Res 1996; 224:63–71.
65 Eizirik DL, Bjorklund A, Welsh N: Interleukin-1-induced expression of nitric oxide synthase in insulin-producing cells is preceded by c-fos induction and depends on gene transcription and protein synthesis. FEBS Lett 1993;317:62–66.
66 Ohta M, Tarnawski AS, Itani R, Pai R, Tomikawa M, Sugimachi K, Sarfeh IJ: Tumor necrosis factor alpha regulates nitric oxide synthase expression in portal hypertensive gastric mucosa of rats. Hepatology 1998;27:906–913.
67 Dupraz P, Cottet S, Hamburger F, Dolci W, Felley-Bosco E, Thorens B: Dominant negative MyD88 proteins inhibit interleukin-1beta /Interferon-gamma-mediated induction of nuclear factor kappa B-dependent nitrite production and apoptosis in beta cells. J Biol Chem 2000; 275:37672–37678.